15th Australasian Fluid Mechanics Conference
The University of Sydney, Sydney, Australia
13-17 December 2004

The External Flow Structure of a Naturally Precessing Fluidic Jet

Chong Y. Wong[1], Richard M. Kelso[1] and Graham J. Nathan[1]

[1]School of Mechanical Engineering
The University of Adelaide, Adelaide, SA, 5005 AUSTRALIA

Abstract

A novel direction and phase-triggered Particle Image Velocimetry experiment has been applied to the near external field of a fluidic precessing jet nozzle. The results reveal significantly more detail of the flow structure than has been known previously. In particular three main vortex pairs which may contribute to the unsteady and mixing characteristics of the external fluid have been identified for the first time.

Introduction

Unsteady precessing flow instabilities can occur within an axisymmetric nozzle of appropriate geometrical dimensions. They are of interest fundamentally because the mechanisms which generate them are still poorly understood. In practice, their occurrence can either be undesirable, as in milk driers [1] or desirable when applied to the combustion of gaseous and particulate fuels in a precessing jet burner [2]. The main advantage of the precessing jet burner lies in its mechanical simplicity, increased flame radiation and its low-NO_x capabilities. Although this type of burner has been used since the early 1990s, the details of the underlying mechanism and structure of the external flow have yet to be identified.

Measurements of the external flow structure from fluidic precessing jet nozzles are limited. Nathan, Hill & Luxton [3] provided information on both the internal and external flow structure of a simple nozzle configuration (Figure 1) that produces a precessing jet. They deduced key features of the flow based on information from various flow visualisation techniques, such as China-clay surface flow visualisation, coloured dye visualisation, bubble visualisation and smoke visualisation. However, no quantitative information of the instantaneous flow structure could be obtained from their techniques.

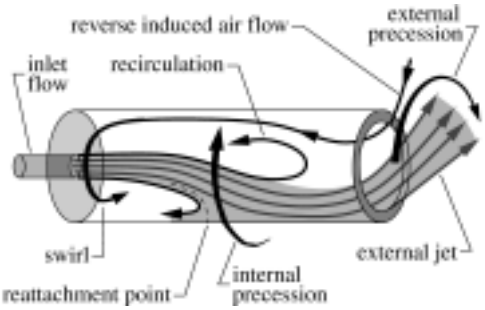

Figure 1. Flow-field of a fluidic precessing jet (Wong *et al.* [4]).

From the flow visualisation results of Nathan *et al.* [3], Kelso [5] analytically proposed that the internal jet precession is sustained by a "driving vortex" just downstream of a sudden expansion with a diameter expansion ratio of D/d=5. Computational fluid dynamic simulation by Guo *et al.*[1] for the same expansion ratio in a long downstream pipe at $Re_d=10^5$ also revealed the motion of an internal precessing jet that generates similar surface flow patterns observed in a shorter downstream chamber used by Nathan *et al.* [3].

Newbold *et al.* [6] employed cross-correlation digital Particle Image Velocimetry (PIV) with a continuous Argon-ion laser beam modulated with an acousto-optic modulator on a fluidic precessing jet (FPJ) nozzle with a lip-and-centrebody arrangement. Due to the constraints of their optical arrangement their data suffered from severe out-of-plane particle movement. Hence, no details of the velocity near to the nozzle exit could be obtained from that investigation. However, an instantaneous image pair in the far-field appears to indicate some regions of flow reversals on the nozzle centreline, consistent with jet precession.

Nobes *et al.* [7] improved on the spatial resolution of the PIV arrangement and details of the flow near to the exit of the PJ could be quantified and studied. However, since their experiments were not phase-averaged, little can be said about the structure of the external jet.

Wong *et al.* [8] visually sorted their free-running PIV data into either a left-sided, or right-sided emerging precessing jet. They reported that the spatially-averaged emerging precessing jet has a centreline decay that is more rapid than a free turbulent jet with a uniform initial velocity distribution. However, their results suffered from directional ambiguity of the emerging jet.

The present paper describes an experimental technique which allows the emerging precessing jet to be directionally resolved and phase-averaged. Phase averaging the emerging jet reveals finer aspects of the 'instantaneous' precessing flow than has been previously studied.

Experimental Details

Details of the FPJ nozzle and the phase-triggered PIV system are shown in Figure 2. The flow at the inlet plane is seeded with 1μm olive oil droplets and has a flat velocity distribution [4,8] with an inlet velocity u_i=55.0 m/s giving a Reynolds number of Re_d=59,000. At this velocity, the precession frequency, f_p, is approximately 6Hz, giving a Strouhal number, St_d=0.0017 based on u_i and d.

A pair of hot-wire (HW) anemometer probes (each being 1mm long Wollaston wire of 5mm nominal diameter) are positioned just downstream of the exit lip. The centre of the lag HW was located at $x'/D_2=0.15$ (D_2=64mm and refers to the exit lip diameter) and $r/D_2=0.58$ and was azimuthally offset from the lead HW by 24°. Both wires were previously adjusted to respond equally to the same flow before the offset was applied.

The signals from each HW are low-passed filtered at a cut-off frequency of 30Hz and passed into respective Schmitt Triggers (STs). These triggers output a high signal (+5V) each time the filtered signals exceed an arbitrary upper trigger voltage level (2/3 of +5V) and they output a low signal only if the input signal falls below a pre-determined lower trigger level. Fluctuating signals between these two ranges are ignored by the trigger.

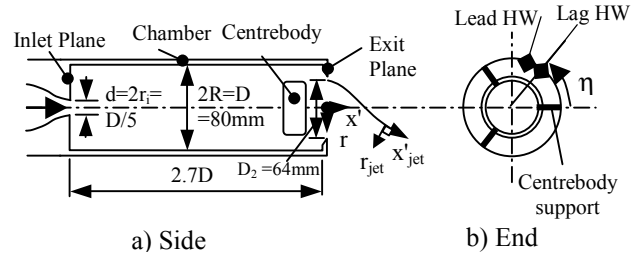

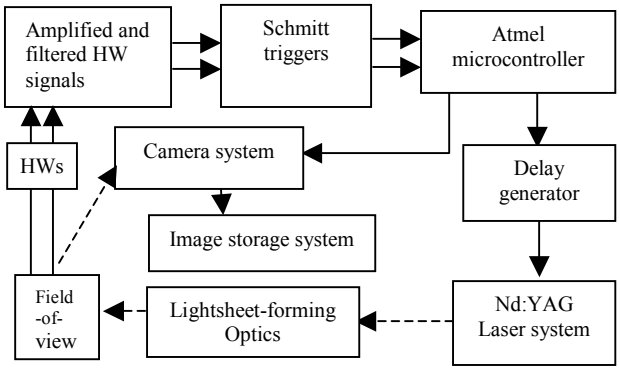

Figure 2. Details of the FPJ nozzle and the PIV system (solid and dashed arrows refer to electrical and light signals respectively).

The outputs from the Schmitt triggers are fed into the interrupt inputs of an 8-bit Atmel AT90S2313-10PC programmable microcontroller. This controller is responsible for generating a constant train of 10Hz pulses to a Stanford Research Systems pulse delay generator (DG-535) which regulates the flashlamp and Q-switch timing of a Quantel Brilliant Twins Nd:YAG laser operating at a wavelength of 532nm with a power of 180mJ per oscillator output. The output laser beam passes through a series of optical lenses to produce a lightsheet that is approximately 2 mm thick in the region of interest.

When the microcontroller determines that the lag ST is triggered after the lead ST and this event occurs within 2.5ms of the next laser clock pulse, the microcontroller activates the camera to record a pair of PIV images. In this way, only one precession direction is selected. A Kodak Megaplus ES1.0 camera which has an array of 1018 by 1008 pixels is used with an AF Zoom-Nikkor 70-300mm f/4-5.6D ED lens at an f# of 5.6.

A total of 11 transverse planes (x'/D_2=0.11,0.19, 0.27, 0.34, 0.42, 0.50, 0.58, 0.74, 0.89, 1.05 and 1.20) were measured. The time interval between each laser pulse varies with distance downstream from the exit lip. It was 15µs for $0<x'/D_2<0.58$, 30µs for $0.58\leq x'/D_2\leq 0.89$ and 20µs for $x'/D_2>0.89$. An interrogation window size of 32 by 32 pixels with a 50% overlap was used (measurement volume is 6.3mm × 6.3mm × 2mm). A total of 12 planes (η = 0°, 15°, 30°, 45°, 60°, 75°, 90°, 105°, 120°, 135°, 150°, 160°) were also interrogated in the longitudinal section, this time using an interrogation window size of 16 by 16 pixels (measurement volume is 1.51mm × 1.51mm × 2mm) and zero overlap. The time interval used here was 15µs. Velocities from all the image pairs were calculated using PIVview 1.7's cross-correlation algorithm.

Results

Nominally 50 instantaneous image pairs were averaged in each experimental plane. Axial vorticity results from each transverse section and tangential vorticity results from each longitudinal section are presented in Figures 3 and 4 respectively. The jet in Figure 3 is precessing in a clockwise fashion, while the jet to the right of r/D_2=0 in Figure 4 is moving out of the page.

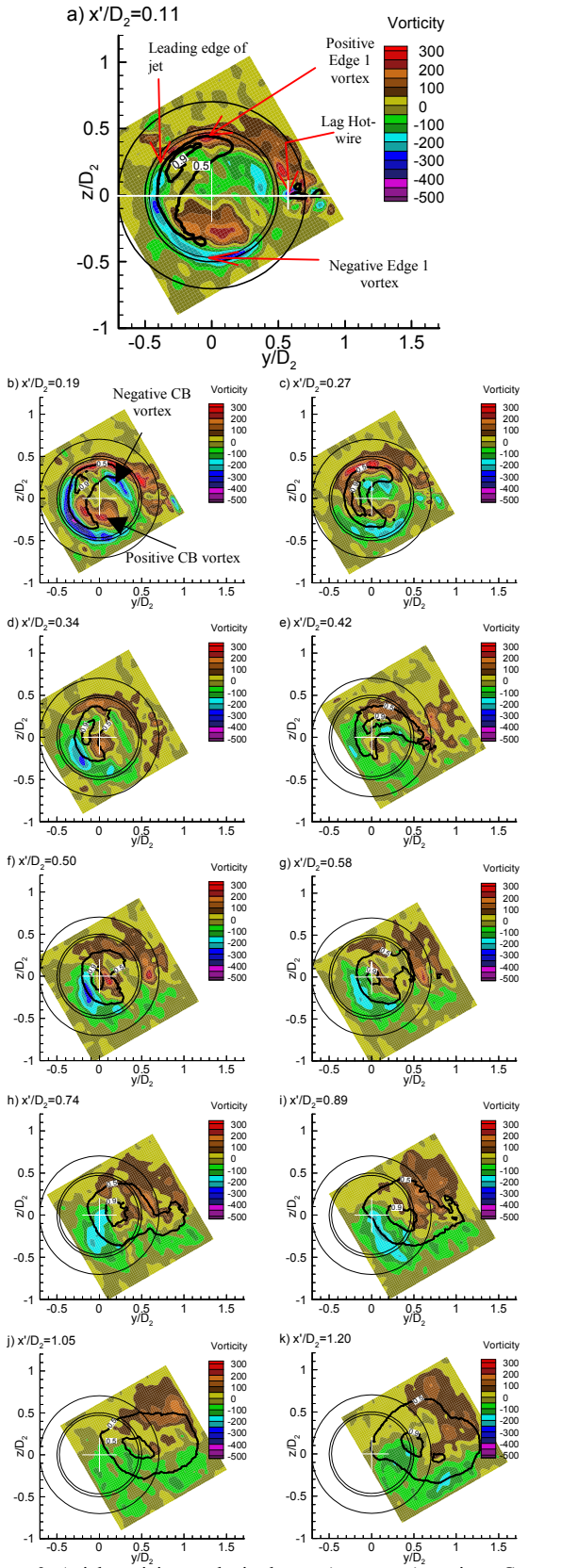

Figure 3. Axial vorticity results in the y-z (transverse) section. Contours representing 0.5 and 0.9 $(v^2+w^2)^{1/2}_{max}$ are overlaid on the coloured vorticity contours.

In Figure 3(a), a pair of vortices can be observed near to the central axis of the nozzle. Results from surface flow visualisation (Figure 5) of a non-precessing deflected jet using the same nozzle confirms that these central vortices (CB vortex pair) originate from a pair of foci on the downstream face of the centrebody. The CB vortices move closer to each other with downstream distance and finally annihilate each other by x'/D_2~0.5 (Figure 6), or possibly reconnect to form a closed loop.

Another pair of vortices surrounding the CB vortices is also apparent. The 'legs' of this vortex form a pair of longitudinal vortices downstream from the centrebody. These appear as negative and positive vorticity regions as seen by a downstream observer. These vortices which depart the centrebody at an inclined angle ('Edge 1' vortex pairs) are thought to originate from the outer edges of the centrebody. Thus, this vortex pair appears as two kidney-shaped patterns near to the exit plane. The negative edge of this vortex initially follows the trajectory of the main jet fairly closely, but at x'/D_2=0.58, it departs, with increasing radius from the nozzle axis, in a direction opposite to the jet precession.

A third vortex pair is also found to sit slightly above the surface of the exit lip. It then lifts away from the lip at the rear side of the exiting jet at the position of the lag-hot-wire probe in figure 3a, approximately 130° to 150° from the centre of the emerging jet. This range of angles is similar to the separation angles of the surface flows in jets in cross flows [9]. The vorticity associated with this vortex pair ('Edge 2 Vortex') is labelled (Fig. 4a) and is most clearly seen in all of Figure 4. The trajectories of the two 'legs' of this vortex pair follow the same trend as the 'Edge 1' vortex pair (in terms of the y-z trajectory with downstream distance) albeit with a slight delay in phase. The presence of this vortex pair below the core of the jet was also detected in earlier phase-averaged LDA studies [4].

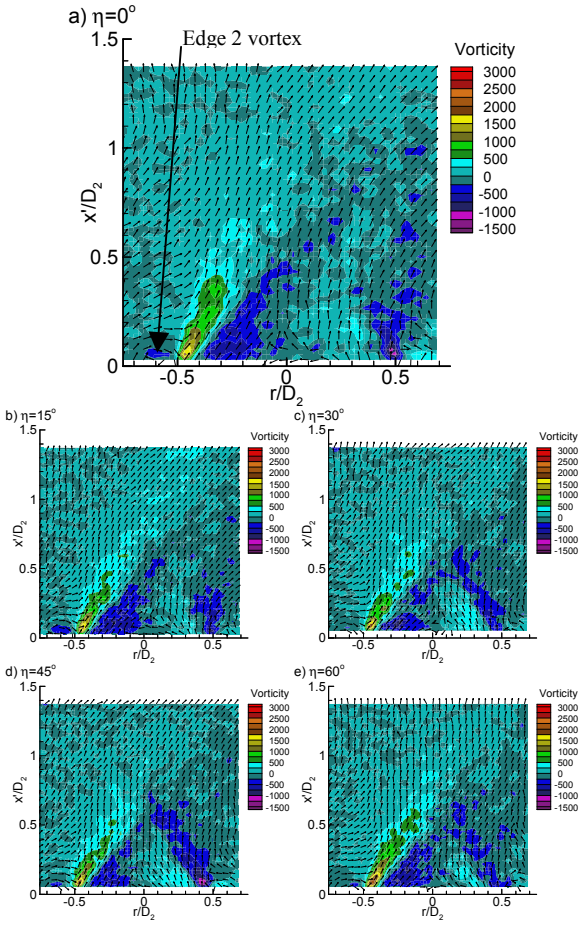

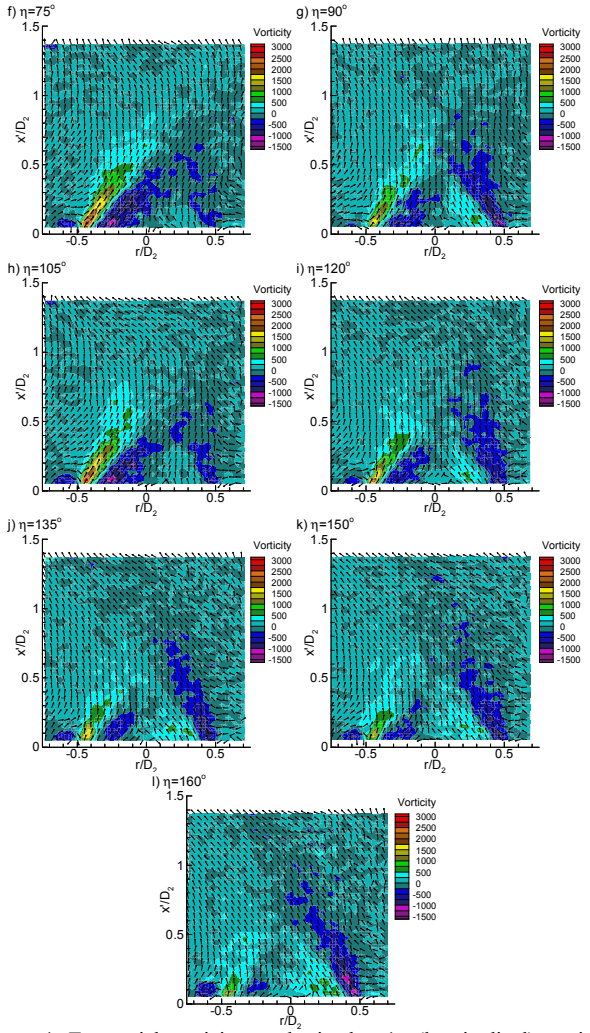

Figure 4. Tangential vorticity results in the x'-r (longitudinal) section. Velocity vectors indicate direction only.

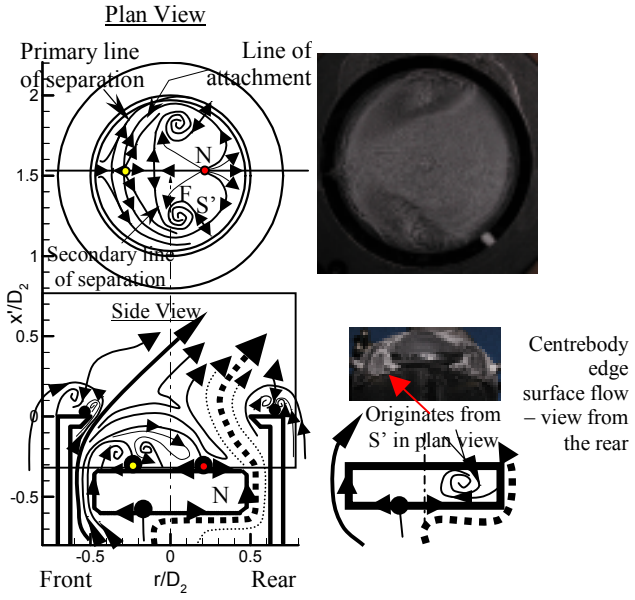

Figure 5. Pre-exit lip flow topology interpreted from PIV and surface flow visualisation experiments (top-right). Not to scale.

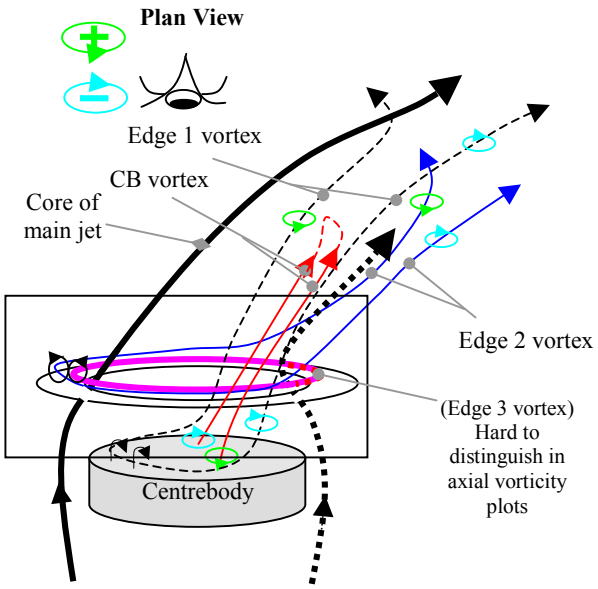

Figure 6. Overall flow topology interpreted from PIV and surface flow visualisation experiments.

Adjacent to the 'Edge 2 Vortex' is an 'Edge 3 Vortex' with a different sign of vorticity (at approximately r/D_2=0.5 in Figure 4). This vortex is relatively small just off the edge of the field of view and Figure 6 illustrates the qualitative location of this small feature. Due to its small size, it is not further discussed here.

Interpretation of results

By combining the PIV and surface flow visualisation results, the external structure of the precessing jet is qualitatively constructed as shown in Figures 5 and 6.

Conclusions

The phase-averaged structure of an external precessing jet is revealed, for the first time, by means of a novel PIV experimental technique which resolves the phase and direction of the naturally precessing jet. The study found that at least three large-scale fluid vortex pairs exist in this flow:

- a 'Centrebody' vortex pair that originates from the foci on the downstream face of the centrebody;
- an 'Edge 1' vortex pair surrounding the inner 'CB vortex pair' and likely to originate from the edge of the centrebody, and
- an 'Edge 2' vortex pair that orignates from the top surface of the exit lip.

A fourth vortex pair adjacent to the top surface of the exit lip is also deduced to be present, however, due to its small size, it is not examined further.

Acknowledgments

CYW is thankful for the International Post-graduate Reseach Scholarship and the Adelaide University Scholarship. The help from Mr. Owen Lucas, who assisted in writing the code for the microcontroller, is also acknowledged. The facilities from the Turbulence, Energy and Combustion Group (The University of Adelaide) have been developed with support from the Australian Research Council, The University of Adelaide and FCT-combustion through the LIEF, LARGE and SPIRT grant schemes.

References

[1] Guo, B.Y., Langrish, T.A.G., Fletcher, D.F., Numerical simulation of unsteady flow in axisymmetric sudden expansions, *Trans. ASME: J. Fluids Eng.*, **123**, 2001, 574-587.

[2] Manias, C.G., Nathan, G.J., Low NO_x clinker production, *World Cement*, **25**(5), 1994, 54-56.

[3] Nathan, G.J., Hill, S.J. & Luxton, R.E., An axisymmetric 'fluidic' nozzle to generate jet precession, *J. Fluid Mech.*, **370**, 1998, 347-380.

[4] Wong, C.Y., Lanspeary, P.V., Nathan, G..J., Kelso, R.M. & O'Doherty, T., Phase averaged velocity in a fluidic precessing jet nozzle and in its near external field, *J. Experimental Thermal and Fluid Science,* **27**, 2003, 515-524.

[5] Kelso, R.M., A Mechanism for jet precession in axisymmetric sudden expansions, in Proc. *14th Australasian Fluid Mechanics Conference*, editor B.B Dally, Adelaide, Australia, **2**, 2001, 829-832, 10-14 Dec.

[6] Newbold, G.J.R., Nobes, D.S., Alwahabi, Z.A., Nathan, G.J. & Luxton, R.E., The application of PIV to the precessing jet nozzle, in *Proc.12th Australasian Fluid Mechanics Conference*, editor R.W. Bilger, Sydney, Australia, **1**, 1995, 395-398, Dec.

[7] Nobes, D.N., Newbold, G.J.R., Hasselbrink, E.F., Su, L., Mungal, M.G. & Nathan, G.J., *PIV and PLIF measurements in precessing and round jets*, Internal Report, Dept. Mech. Engng., University of Adelaide, Australia, 2002.

[8] Wong, C.Y., Nathan, G.J. & Kelso, R.M., Velocity measurements in the near-field of a fluidic precessing jet flow using PIV and LDA, in *Proc. 3rd Australian Conference on Laser Diagnostics in Fluid Mechanics and Combustion,* Uni. of Queensland, Brisbane, Australia, Paper 4, 2002, 48-55, 2-3 Dec.

[9] Fric, T.F., Roshko, A., Vortical structure in the wake of a transverse jet, *J. Fluid Mech.*, **279**, 1994, 1-47.